Impact of the Heat Source Selection on the High Temperature Electrolysis Performances and Economic Competitiveness

Article · January 2004

Source: OAI

CITATIONS
0

READS
321

3 authors:

Rodrigo Rivera Tinoco
Pentair - Haffmans
55 PUBLICATIONS **599** CITATIONS

SEE PROFILE

Christine Mansilla
Atomic Energy and Alternative Energies Commission
76 PUBLICATIONS **1,226** CITATIONS

SEE PROFILE

Chakib Bouallou
MINES ParisTech
145 PUBLICATIONS **2,963** CITATIONS

SEE PROFILE

Energy Conversion and Management 51 (2010) 2623–2634

Contents lists available at ScienceDirect

Energy Conversion and Management

journal homepage: www.elsevier.com/locate/enconman

Competitiveness of hydrogen production by High Temperature Electrolysis: Impact of the heat source and identification of key parameters to achieve low production costs

R. Rivera-Tinoco [a,b], C. Mansilla [b], C. Bouallou [a,*]

[a] MINES ParisTech, Centre Energétique et Procédés, 60 bd. Saint Michel, 75006 Paris, France
[b] Commissariat à l'Energie Atomique et aux Energies Alternatives, CEA, DEN, I-tésé, F-91191 Gif-sur-Yvette, France

ARTICLE INFO

Article history:
Received 4 September 2009
Accepted 27 May 2010
Available online 23 June 2010

Keywords:
High Temperature Electrolysis
Techno-economics
Heat source
Hydrogen

ABSTRACT

Among the more efficient and sustainable processes that are studied for massive hydrogen production, High Temperature steam Electrolysis seems a promising process. When operating in the autothermal mode, this process does not require a high temperature source for the electrolysis reaction but only a thermal energy source able to supply enough heat to vaporize water. Using a simplified economic model, we assess the impact of the temperature, pressure and thermal energy cost of the heat source on the process competitiveness. Results show that medium temperature thermal energy sources could be coupled to the High Temperature Electrolysis process without resulting in strong overcosts. Besides, key parameters are also identified among the electrolyzer characteristics. Relevant results indicate that R&D on electrolysis cells must continue focusing on the lifespan of these equipments, for which a target lifespan of 3 years could be established.

1. Introduction

Among the several processes currently studied, the perspective of higher efficiencies on hydrogen massive production aroused particular interest for High Temperature Electrolysis (HTE), which since the early 1980s has demonstrated thermodynamic advantages of steam electrolysis (at temperatures above 1023 K up to 1223 K) over liquid water [1]. Besides, on an environmental basis, Life Cycle Assessment results presented by Utgikar and Thiesen [2] and Lattin et al. [3] show HTE as a potential process driving towards hydrogen production with lower carbon dioxide emissions, especially when being fed by nuclear electricity and compared to Steam Methane Reforming (SMR).

Up to now, studies about the coupling of the HTE process with high temperature energy sources, such as the Very High Temperature nuclear Reactor (VHTR), have been carried out mainly suggesting the use of heat for the steam production and overheating, and for the electrolysis reaction [4–6]. However, providing this energy to the electrolyzer is yet to be technically demonstrated. Otherwise, when electrolyzers operate in autothermal mode (i.e. electricity-only operation), the process does not require a high temperature source. Consequently, recent works consider thermal energy sources with lower operating temperatures only for water vaporization. Sigurvinsson et al. [7] proposed the use of geothermal energy to produce steam further overheated in a heat exchanger network that recovers the heat from the oxygen and hydrogen streams exiting the electrolyzer (Fig. 1).

McKellar et al. [8] studied the coupling between HTE process and a Sodium Fast Reactor (SFR), which operates at lower temperatures than VHTRs. The water circuit of the reactor operating at 700 K supplies the heat needed to vaporize water for the HTE process, which reaches 529 K and is overheated afterwards up to the optimal temperature by recovering process heat. Once the heat from the hydrogen stream is recovered, the hydrogen mixed to remaining steam is separated by flash separators.

These works dealing with medium or low temperature energy sources enable to enlarge the list of thermal energy sources to be coupled with the HTE process. However, not all of them would be able to supply enough energy to produce steam in large amounts or be suitable because of their intrinsic economic variables. Therefore, this work on techno-economics of massive hydrogen production by HTE firstly focuses on the impact on the hydrogen production cost of technical issues such as the steam generation and thermal energy sources, and secondly focuses on the impact of the electrolysis cell lifespan and current density, as well as economic factors such as electricity and thermal energy costs, electrolysis cells investment cost and economies of scale.

In order to assess the impact of the heat source and electrolyzer characteristics as previously mentioned, we first perform the economic modeling of the process, which enables to calculate the

* Corresponding author.
E-mail address: chakib.bouallou@mines-paristech.fr (C. Bouallou).

0196-8904/$ - see front matter © 2010 Elsevier Ltd. All rights reserved.
doi:10.1016/j.enconman.2010.05.028

Nomenclature

A	section, m^2
Cap	production capacity, items/yr
C_i	cost, €
c_i	unitary cost, €/m^2, €/kW, €/kW h
Cp_i	specific heat from gas, kJ/kg K
CTA	hydrogen production cost, €/kg
Dh	hydraulic diameter of the heat exchanger, m
E	electric potential, V
E°	standard electric potential, V
F	faraday constant, 96,500 C
f	friction factor
FS	entropy factor, V
h_c	height of the electrode channel, m
H_t	annual production of hydrogen, kg/yr
I_i	investment, €
j	electric current density, A/m^2
l	cell width, m
L	cell length, m
M_i	molecular weight, g/mole, kg/kmole
$\dot{m}_i$	mass rate, kg/s
NP	number of plates in the exchanger
PW_i	power, MW, kW, W
$\dot{Q}_i$	thermal power, kW, W
T	temperature, K
tx	partition ratio
W_i	work, MW

Greek symbols

ΔE_l	overpotential, V
ΔP	pressure drop, Pa
ε	reaction yield
ρ_i	mass density, kg/m^3
τ	discount rate, %
τ_i	thickness, m

Indexes

atm	atmospheric
act	activation
anode	anode
BP-TURB	low pressure turbine – SFR
B(X)–ent(Y)	exchanger *X*, inlet of fluid *Y*
B(X)–sort(Y)	exchanger *X* outlet of fluid *Y*
cathode	cathode
cell	electrolysis cell
compress	compressor
conso,elec	electric consumption
conso,th	thermal consumption
conc	concentration
electrolyte	electrolyte
flash	flash separator
H_2	hydrogen
HP-TURB	High Pressure turbine – SFR
i,flash	flash separator investment
i,rectifiers	current rectifier investment
i,transf-MT	mid-voltage transformer investment
i,transf-LT	low-voltage transformer investment
ielec	electrolysis zone investment
i,electrol	electrolyzer investment
inelec	electrolyzer inlet
inv,base,pump,i	investment base cost of pump *i*
inv,base,compress	investment base cost of compressor
kWhe	kiloWatt-hour electric
kWhth	kiloWatt-hour thermal
Na-loop	sodium loop of the SFR
ohm	ohmic
op,electrol	operating of electrolyzer
op-HX,i	operating of heat exchanger *i*
op,SX	operating of overheater SX
pump,i	pump *i*
PUMP1	pump 1 of SFR
PUMP2	pump 2 of SFR
steam	water steam
sys	system
tot	total

hydrogen production cost based on the physical modeling and component design of the process equipments. Finally, the HTE key parameters, trends and R&D targets for driving this process towards competitiveness are described.

2. Process flowsheet

The flowsheet here studied is based on different previous studies and is presented in Fig. 2. The demineralized water fed into the process (stream INH2O) is firstly preheated in the heat exchangers B7 and B8 before being vaporized by using the thermal energy supplied by the selected source. After steam generation, the steam stream is divided into two streams which are connected to a heat recovery network, as presented by Sigurvinsson et al. [7]. In the heat exchangers composing this network (named B1–B4) the steam is overheated by means of the recovered energy from hydrogen–water and oxygen streams exiting the electrolyzer. The heat exchangers are assumed to be plate type. At the outlet of this network, the temperature of the overheated steam is eventually increased by means of an electric heater (SX) that allows the steam to reach the optimal temperature at the inlet of the electrolyzer. From the electrolyzer outlet, part of the hydrogen produced is directed again to the electrolyzer inlet in order to reach a hydrogen concentration of at least 10%mol which avoids corrosion of the cathodes [9]. Also 50% of the oxygen at the outlet is recycled to the anode inlet as a sweep gas used to evacuate the oxygen produced by the electrochemical reaction [10]. Finally, we included a purification system consisting on flash vessels in which the hydrogen that exits the heat recovery network is separated from the remaining steam. Purified hydrogen is then compressed (B13) to the required delivery pressure [8,11,12].

3. Energy sources

3.1. Thermal energy sources

In previous works [13,14], we dealt with the potential for steam production of thermal energy sources of two different kinds: those involving incineration units, specifically the combustion of biomass and domestic wastes, and the development of techniques to produce steam by using the European Pressurized nuclear Reactor (EPR) and Sodium Fast nuclear Reactor (SFR). In the incineration units, the steam is generated conventionally inside the combustion chamber. As regards the EPR, steam is generated in the secondary loop that normally feeds the turbines with saturated steam in order to generate electricity. The coupling of this reactor with HTE assumes the drawing off of part of the steam generated in the

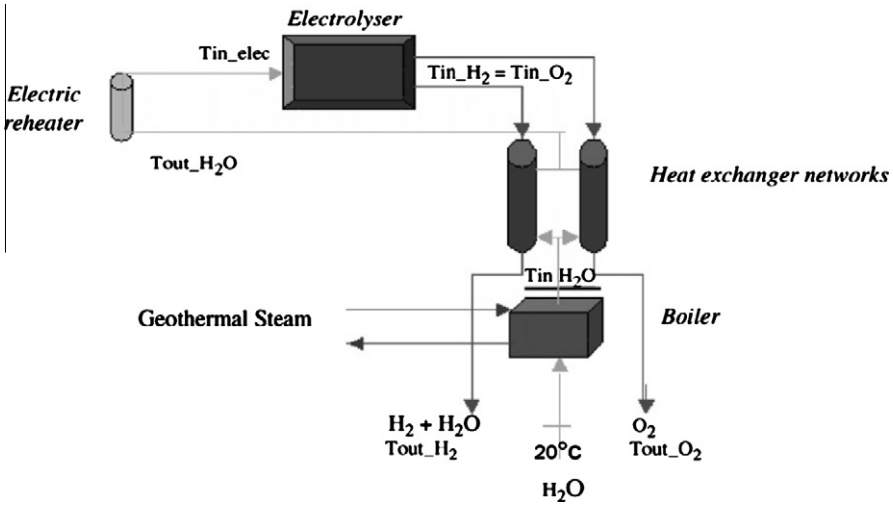

Fig. 1. HTE coupled to geothermics [7].

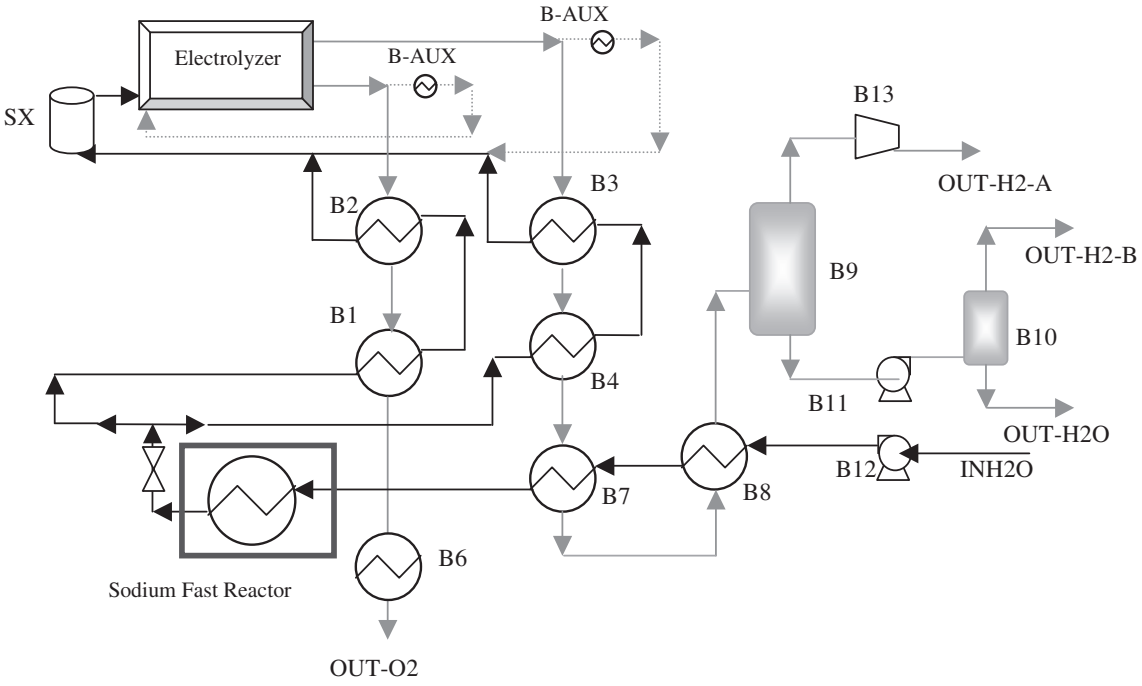

Fig. 2. Flowsheet of the High Temperature Electrolysis process.

mentioned loop and its directly introduced into the heat exchanger network.

The steam production by using the SFR also considers the drawing off of the steam from the steam loop. However, since this coupling is somewhat trickier, we extensively studied the steam production by simulating the water loop of the reactor in ASPEN Plus® and accounting for its operating parameters [15]. We proposed three steam generation techniques placed as shown in Fig. 3. Due to safety issues, it is strongly recommended not to generate additional steam by adding exchangers on the sodium loops [15].

The impact of each steam production technique was evaluated by estimating the variation on the electricity generation efficiency (Eq. (1)). For this purpose, we considered the heat exchanged between the sodium and water loops ($Q_{Na\text{-}loop}$), the energy needed to pump the water for the reactor (W_{Pump}) and the power obtained in both turbines (W_{Turb}). Results were found within the range of values presented in the literature for SFR efficiency [15–17].

$$\eta_{rend} = \frac{W_{HP\text{-}TURB} + W_{BP\text{-}TURB} - W_{PUMP1} - W_{PUMP2}}{Q_{Na\text{-}loop}} \quad (1)$$

The first technique for steam production consists in a direct drawing off while additional liquid water counterbalances the steam drawn off (Fig. 4). The pressure and temperature at the High Pressure turbine outlet are 2.0 MPa and 484 K respectively. At these operating conditions, steam could be directly introduced to the HTE heat recovery network. However, the rate of the steam drawing off must not disturb the reactor functioning. Therefore, we estimated the limiting rates in four steps:

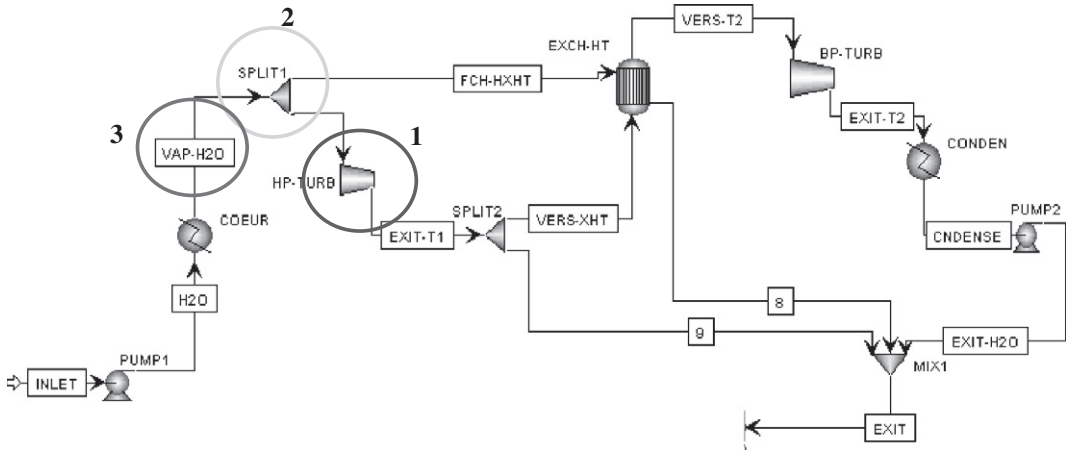

Fig. 3. Sodium Fast Reactor – water loop flowsheet and steam generation for HTE process.

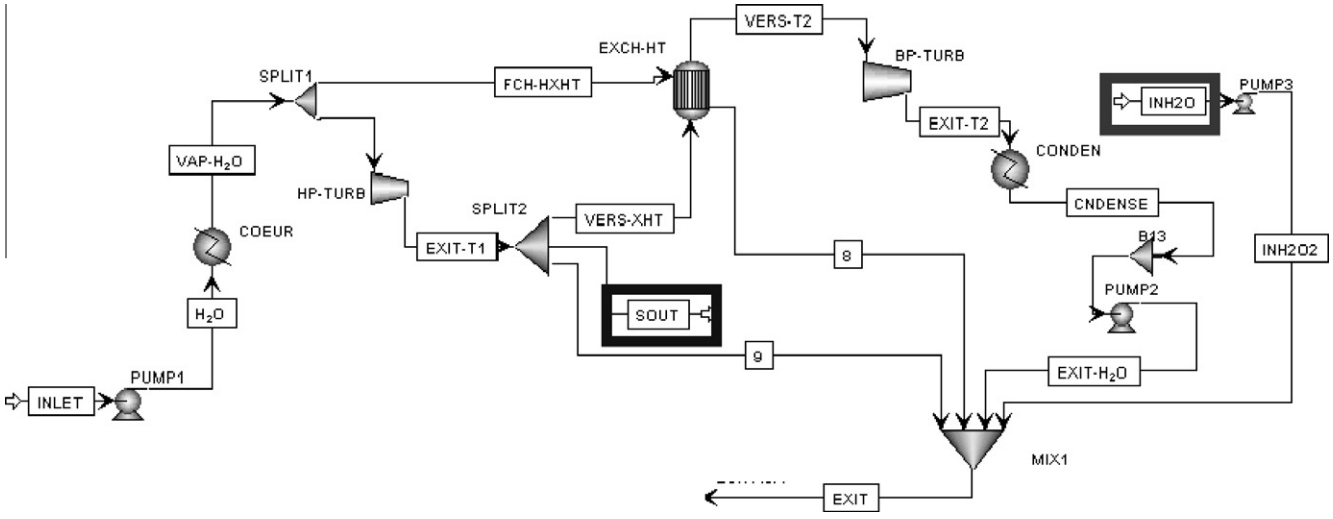

Fig. 4. Steam drawing off after the High Pressure turbine.

A. The drawing off of the steam is performed at the outlet of the High Pressure turbine (HP-TURB) until being near and before the risk of malfunctioning of the reactor, without modifying the rate of the steam sent to the Low Pressure Turbine (BP-TURB) or any other stream than stream 9 (see Fig. 4).
B. The drawing off of the steam is carried out at the outlet of the High Pressure turbine (HP-TURB) but also by lowering the steam rate sent to the low pressure turbine (VERS-XHT stream).
C. Once the limiting rate of *B* case is reached, further drawing off of the steam is carried out at the outlet of the High Pressure turbine (HP-TURB). However, the steam rate sent to the heat exchanger EXCH-HT through the stream FCH-HXHT is also lowered.
D. The counterbalance water feed is firstly introduced at 333 K (INH2O). We performed a sensitivity study by assuming higher temperatures in order to assess their influence on the reactor functioning.

Table 1
Maximal steam rate available from a SFR – direct drawing off of steam.

Sodium fast reactor as a thermal energy source	Case *A*	*B*	*C*	*D*
Maximal steam rate drawn off (kg/s)	12	60	69	69
Maximal hydrogen production (kg/s)	1.3	6.7	7.7	7.7
Efficiency drop on the reactor (%)	0.1	1.2	1.8	1.6

The efficiency reduction results for each case are presented in Table 1. The drawing off of the *A* case has the lowest influence on the reactor behavior, especially because it has no direct link with the operating conditions of the low pressure turbine (BP-TURB), which produces more than 60% of the electricity. The maximal value that could be reached leads to a hydrogen production of 7.7 kg/s, assuming total conversion from steam into hydrogen in the global HTE process. The electricity power needed for the electrolyzer in this case is estimated at 1000 MW.

The second technique is similar to the proposal presented by McKellar et al. [8] and appeals to an external heat exchanger that will be supplied with some steam, as the hot-fluid, coming from the water loop of the reactor (see Fig. 5 – left). The cold-fluid would be liquid water to be vaporized. Assuming that the decrease in temperature from the steam reaches 100 K, a maximal rate of steam of 26 kg/s could be obtained. This rate is almost three times lower than the one presented in the above paragraph and it would lead to the same efficiency decrease of 1.6%.

The third technique consists in introducing a heat exchanger at the outlet stream of the steam generator of the reactors (see Fig. 5 – right). All the steam flowing in the reactor's water loop is introduced into the exchanger and cooled down by maximum 10 K. Liquid water is vaporized with the heat supplied by the steam and is afterwards introduced in the heat recovery network of the HTE process. This technique allows limited decrease in efficiency and

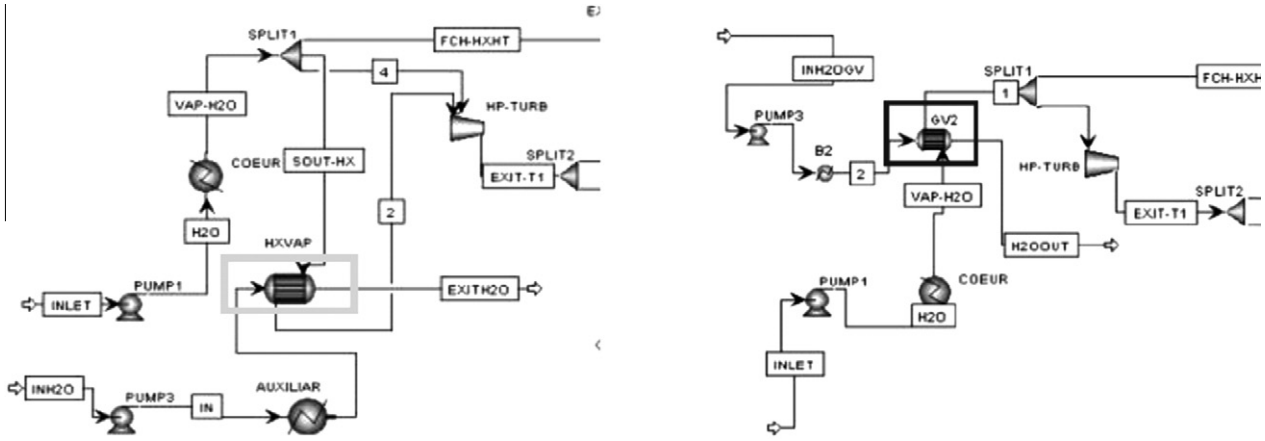

Fig. 5. Steam generation techniques: drawing off to produce steam in an additional heat exchanger (left) and total flow with slight decrease on the temperature of the water loop (right).

maximal hydrogen production at around 0.5% and maximum 1.7 kg/s respectively.

In Table 2 we present the summarized characteristics of the steam produced by the thermal energy sources considered: incineration units of biomass or domestic waste and the two kinds of nuclear reactors. In the case of the SFR, the direct drawing off of steam was retained (i.e. 1st technique) because of its larger potential for massive hydrogen production. For the EPR, we retained two different values for steam properties that result from the safe and feasible range in which the drawing off of steam from the reactor's water loop could be carried out.

As this study focuses on the competitiveness of the HTE process, the cost values of the thermal energy produced by the sources retained are needed to evaluate hydrogen production costs. As it was detailed in previous works [4,13], we estimate the thermal energy costs from incineration units by sizing them as a function of the hydrogen production capacity. For nuclear reactors, this cost is estimated as a function of the electricity cost and the efficiency of the reactor. Specific values are presented further in this work.

3.2. Electric energy source

For HTE, as for all other electrochemical processes, electrical energy supply is a major issue. Several means could be considered: supplying the process with electricity from the grid or coupling the HTE process to a dedicated power plant. This will derive from the business model to be implemented. This work will strictly focus on the heat source and the study of the influence of the electricity cost on the hydrogen production cost rather than possible business model development. For the reference case, a cost of 40 €/MW h will be used, assuming it corresponds to a dedicated nuclear plant.

4. Techno-economics of the process

4.1. Equipment design, investments and operating costs

In this section, we present the technical and economic modeling of the process equipments, which allow us to estimate the investment and operating costs. From a technical point of view, the modeling of the electrolyzer was carried out considering the Nernst equation with the overpotentials generated in the electrolysis cells. For the other equipments (heat exchangers, pumps, compressor and flash separators), classical methods were used: such as the LMTD for the heat exchanger design. Concerning the economic part, the heat exchangers, pumps and compressor investment costs were estimated by the Chauvel method [10,18], whereas a target cost from the literature was selected for the electrolyzer.

4.1.1. Electrolyzer

The electrochemical reaction takes place inside reversible Solid Oxide Electrolysis Cells (SOECs), operating over 1023 K [19]. In order to estimate the electric potential of the cell and the energy needs, the modeling of the phenomena inside the cell is performed considering planar rectangular SOECs, because of their flexibility, compactness and easy-production characteristics, as well as numerous works describing their performances [20–22]. The unitary cell studied in this work is presented in Fig. 6 and could be electrolyte or cathode supported. An active surface of 0.04 m^2 is considered [23] and we assumed that cells would be assembled into stacks, composing the electrolyzer.

The Gibbs free energy (ΔG) and the thermal part ($T\Delta S$) needed to convert the steam must be supplied by electricity as no high temperature source is considered. This would lead to three operating modes. First, the endothermal mode is observed when the overpotentials inside the cell (or energy losses) do not supply sufficient energy to maintain the temperature of the gases. As the reaction takes place, the thermal energy for the reaction is taken from the gases and leads to lower temperatures at the cell outlet. Secondly, the isothermal mode corresponds to the equilibrium between the energy losses in the cell and the energy needs, leading to a constant temperature inside the cell. Thirdly, the exothermal mode is achieved when the gas temperature at the outlet of the cell is higher than at the inlet. Besides, several works have shown that the cell performance and temperature change when they are stacked. However, we assume that the cells in the stack are independent because in future developments, the target is to avoid or minimize these interactions [24,25].

Table 2
Properties of the steam produced by the four thermal energy sources retained.

	SFR	EPR	EPR	Biomass	Domestic waste
Steam temperature from each source (K)	484	523	503	623	713
Steam pressure (MPa)	2.0	4.0	3.0	2.0	4.0

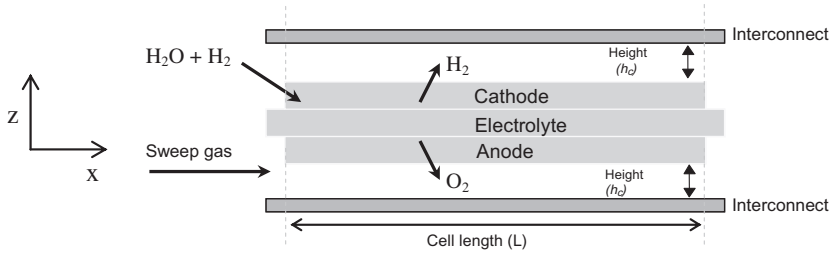

Fig. 6. Unitary cell composing the stack.

In order to estimate the electric potential of the cell and the power needed in the electrolyzer, we assumed that the current density drives the overpotentials and remains constant in the electrodes. The modeling of the cell performance is presented in our previous work [26], in which the electric potential is estimated from the Nernst equation (the equilibrium potential and the corrective factor: $E°$, FS) and the overpotentials of the cell. The phenomena related to these overpotentials are presented in Eq. (2), and correspond to:

- electrodes activation (ΔE_{act}),
- gas concentration in the electrodes (ΔE_{conc}),
- ohmic resistance of the materials from which the cell is made (ΔE_{ohm}).

$$E_{cell} = E^{\circ} + FS + \Delta E_{conc} + \Delta E_{act} + \Delta E_{ohm} \tag{2}$$

The electric power of the electrolyzer (PW_{tot}) needed to reach a given rate of hydrogen ($\dot{m}_{H_2}$) is directly estimated by the electric potential of each cell and the Faraday law (Eq. (3)).

$$PW_{tot} = \frac{2F \times E_{cell}}{1000 \times M_{H_2}} \dot{m}_{H_2} \tag{3}$$

The investment cost for the cells needed in the process is still not available. However, current estimates and target values suggest the value of 170 $/kW [27]. This value does not include installation costs. Moreover, taking into account that the cells present a shorter lifespan value than the one expected for a hydrogen facility, they would need to be replaced and would induce additional investments. We assume replacement costs equal to the first cells investment (Eq. (4)) but discounted and brought up to present values.

$$C_{i,electrol} = 1000 \times PW_{tot} \times 136 \frac{€}{kW} \tag{4}$$

We also take into account the additional costs for the auxiliary equipment of the cells, specifically for the medium (MT) and low (LT) voltage transformers and current rectifiers. Cost data were obtained from the Optimized Program Service, Inc. (OPS), 2004 [10], and are presented in Eqs. (5)–(7) as a function of the power needed in the electrolyzer. The total investment cost of these auxiliary equipments is summarized by Eq. (8).

$$C_{i,transf\text{-}MT} = PW_{tot} \times 13,100 \tag{5}$$

$$C_{i,transf\text{-}LT} = PW_{tot} \times 13,500 \tag{6}$$

$$C_{i,rectifiers} = PW_{tot} \times 16,500 \tag{7}$$

$$C_{ielec} = C_{i,transf\text{-}LT} + C_{i,rectifiers} + C_{i,transf\text{-}MT} \tag{8}$$

The electricity consumption of the electrolyzer is converted into operating cost (€/h) by taking into account the electricity price and the cell electric potential.

$$C_{op,electrol} = \frac{E_{cell} \times 2F \times \dot{m}_{H_2}}{M_{H_2}} \times c_{kWhe} \tag{9}$$

4.1.2. Heat exchangers

Heat exchangers made of corrugated plates were considered to recover the energy from the gases exiting the electrolyzer (B1–B8) [28–30]. The needed surface for each exchanger is estimated by the LMTD method with the thermophysical properties of the gases estimated at the mean temperature of each heat exchanger. Exchangers B1–B4 recover energy from the oxygen and hydrogen-steam streams respectively and allow overheating the water steam produced by the thermal energy source. Exchangers B7 and B8 pre-heat cold water (291 K) before injected into the source. The first of these preheating exchangers drives the temperature of the hydrogen-steam mixture down to the dew point of the mixture, which was evaluated by the Antoine equation. The second exchanger mostly condensates water and cools the mixture down to the operating temperature fixed at 303 K [31] that leads to an almost pure hydrogen stream (>98%mol). Oxygen is also cooled down to the same operating temperature.

As mentioned before, the Chauvel method is used to estimate the installed investment cost of heat exchangers, which is related to the needed materials. Taking into account the process high temperature and gases, two alloys are proposed to build these equipments: INCONEL 601 (beyond 973 K – B2 and B3) and INCONEL 690 (below 973 K – B1, B4, B6, B7 and B8) [10]. The investment unit prices are 1500 and 110 €/m^2 respectively.

Heat recovered in the exchangers is not considered as an energy expense, except for the heat exchanger B6 that cools oxygen. This lost energy represents an operating cost as a contribution to thermal energy expenses (Eq. (10)).

$$C_{op\text{-}HX,B6} = c_{kWhth} Q_{B6} \tag{10}$$

4.1.3. Electric overheater

The outlet temperature of the steam overheated in B2 and B3 is not necessarily the optimal temperature for the electrolyzer operation. This means that the temperature at the electrolyzer inlet could need to be higher in order to obtain lower hydrogen production costs. Therefore, an electric overheater is added, as shown in Fig. 2 (SX). Besides, we assumed the use of auxiliary electric overheaters called B-AUX when the electrolyzer operates in an endothermal mode, as the temperature of the recycled hydrogen and oxygen to the cathode and anode respectively is lower than the one needed at the inlet.

The investment of these equipments is not considered in this work (they are orders of magnitude lower than other investments), contrary to the operating cost. The energy needed to overheat the steam in SX is calculated using the electric energy cost (c_{kWhe}), the steam temperatures and mass flows at the outlet of the heat exchangers B2 and B3 and the optimal temperature at the electrolyzer inlet (T_{inelec}) (Eq. (11)). The energy expenses from the over-

heaters B-AUX are estimated as for SX, but from the electrolyzer outlet temperature and gas flows.

$$C_{op,SX} = \dot{m}_{steam} Cp_{steam} [tx \times (T_{inelec} - T_{B2\text{-}out2}) + (1.0 - tx) \times (T_{inelec} - T_{B3\text{-}out2})] \times c_{kWhe} \quad (11)$$

4.1.4. Pumps

Two pumps made of stainless steel 316 L [10] are used: one (B12) to compensate the steam pressure drops in the heat exchangers and to lead the feeding water from atmospheric pressure (P_{atm}) to the process operating pressure (P_{sys}); and another one (B11) to recycle the water which was not electrolyzed. The pressure drops in each heat exchanger are estimated based on the properties and mass flows of gases, the Reynolds number, friction factors, and exchanger geometry (Eq. (12)). From the pressure drop values, the power of each pump is then estimated adding a 20% safety factor of over-capacity, as presented in Eqs. (13) and (14).

$$\Delta P_i = 2 f \rho_i \left(\frac{\dot{m}_i}{\frac{NP}{2,0} \rho_i A} \right)^2 \frac{1,0}{Dh} \quad (12)$$

$$PW_{pump,B11} = \frac{1.2 \times \dot{m}_i \times \left(\sum_{f.sec} \Delta P_i \right)}{\rho_i} \quad (13)$$

$$PW_{pump,B12} = \frac{1.2 \times \dot{m}_i \times \left(\sum_{f.prim} \Delta P_i + P_{sys} - P_{atm} \right)}{\rho_i} \quad (14)$$

From Paul-Joseph work [10], the investment cost of the pumps was fitted as a function of the pumping power ($PW_{pump,i}$) (Eq. (15)). Operating expenses for the pumping system correspond to electricity consumption and then depend on pumping power, the operating time per year and the electricity cost.

$$C_{inv\text{-}base,pump_i} = 808.19 \times \left(\frac{PW_{pump,i}}{0.98} \right)^{0.2724} \quad (15)$$

4.1.5. Compressor

A compressor is needed in order to reach the hydrogen delivery pressure. In this study, a piston type isentropic compressor made of stainless steel 316 L is considered. The outlet pressure was fixed at 3.0 MPa [31] or 4.0 MPa depending on the inlet pressure of the steam produced by the selected thermal energy source. The inlet pressure in the compressor results from the operating pressure of the process and the pressure drop of the hydrogen-steam mixture through the heat exchangers, which is equivalent to the drop considered for the calculations of B11 pump power. As for pumps, investments and energy consumption expenses are calculated based on the power, operating time and electricity cost.

$$C_{inv\text{-}base,compress} = 16,030 \times PW_{compress}^{0.4411} \quad (16)$$

4.1.6. Flash separators

Liquid and vapor phases with hydrogen and water (generated in the B8 cooler) are assumed to be separated inside the flash separators at isothermal conditions. The calculations of concentration and temperature of the hydrogen-steam phase diagram were performed assuming the PSRK thermodynamic model. Values of equilibrium hydrogen concentration in the liquid and gas phases were used to determine the flow of each chemical compound. In order to determine the flash separator installed investment cost, we fitted the available data for different separators as a function of the inlet stream rate (Eq. (17)), based on Paul-Joseph data [10].

$$C_{inv,flash,i} = 674,697 \times \dot{m}_{flash,i}^{0.4009} \quad (17)$$

4.1.7. Vaporization unit – thermal energy source

As mentioned before, the thermal energy cost is related to the selected source to be coupled with the HTE process. The total expenses depend on the needed energy, which is estimated based on the temperature difference between preheated water and the boiling point at the operating pressure. The investment and operating expenses of the thermal source is implicitly considered in the thermal energy cost.

4.2. Hydrogen production cost

From the investments and operating costs that are detailed in the previous section, the hydrogen production cost can be calculated in €/kg (Eq. (18)) as function of operating conditions. This function is optimized by means of a FORTRAN program of a modified version of the "Adaptive Random Search Method" [32–34] in which the temperatures of the heat exchangers and at the electrolyzer inlet, as well as the flow ratio between the steam sent to recover the heat from oxygen or from hydrogen-steam streams are the optimization variables. Operating pressure was fixed at the same value that the pressure of the steam source.

$$CTA = \frac{\sum_t [((C_{investment})_t + (C_{i,electrol})_t + (C_{conso,th})_t + (C_{conso,elec})_t)(1+\tau)^{-t}]}{\sum_t [H_t (1+\tau)^{-t}]} \quad (18)$$

This function includes the investments cost ($C_{investment}$) of heat exchangers, pumps, flash separators and compressors, the investments of the electrolysis zone as well as the electrolyzer replacement costs ($C_{i,electrol}$) and the operating thermal ($C_{conso,th}$) and electric ($C_{conso,elec}$) energy expenses. The main parameters and economic assumptions of the HTE process are presented in Table 3 and detailed characteristics of the cathode and electrode supported cells considered in this work are shown in Table 4.

5. Results

In order to carry out the impact study of the heat source and other economic factors on the hydrogen production cost, a reference case is firstly defined. It considers the coupling of a Sodium Fast Reactor with the HTE process. For this and further case studies, the optimization of the hydrogen production cost is performed by the "Adaptive Random Search Method" developed for this work. Since some contributions were neglected (electrolyzer installation cost, other investment contributions such as the general facilities or engineering fees, other operating costs such as taxes and insurance), hydrogen production cost values should be considered relatively one to another.

Table 3
Operating parameters and economic assumptions for the HTE process.

Hydrogen production rate, kg/s	1.5
Operating pressure, MPa	2.0–4.0
Steam temperature at thermal source outlet, K	484–713
Outlet oxygen and hydrogen temperature, K	303
Inlet fresh water temperature, K	291
Operating hydrogen pressure (facility outlet), MPa	3.0–4.0
Electrolyzer lifespan, years	5
Conversion yield	0.75
Facility annual availability	80%
Discount rate (τ),	6%
Investment period	3
1st year	15%
2nd year	35%
3rd year	55%
Facility lifespan, years	30
Electricity cost, €/MW h	40

Table 4
Characteristics of cathode and electrolyte supported cells [35,36].

	Electrolyte supported	Cathode supported
Width (l), m	0.1	0.1
Length (L), m	0.4	0.4
Height between interconnect and electrode (h_c), m	1×10^{-3}	1×10^{-3}
Cathode thickness ($\tau_{cathode}$), m	100×10^{-6}	500×10^{-6}
Porosity	0.3	0.46
Tortuosity	6.0	4.5
Anode thickness (τ_{anode}), m	100×10^{-6}	50×10^{-6}
Porosity	0.3	0.3
Tortuosity	6.0	5.4
Electrolyte thickness $\tau_{electrolyte}$), m	1000×10^{-6}	20×10^{-6}
Radio of the electrode pores, m	5×10^{-7}	10×10^{-7}
Operating temperature, K	1023–1273	1023–1223
Hydrogen molar fraction at the electrolyzer inlet	0.1	0.1
Conversion yield (ε)	0.8	0.8
Current densities (j), A/m^2	500–4000	3500–8500

5.1. Reference case: HTE coupled to a SFR nuclear reactor

In Table 5, specific assumptions and results from the optimization of the SFR–HTE coupling are presented. The optimal temperature estimated at the cell inlet is around 1077 K, which corresponds to literature data [8]. The energy recovered from the mixture hydrogen-steam coming from the electrolyzer outlet is more important than from oxygen. This lets us assume that for the optimization most of the steam should be driven to the exchangers B3 and B4 in order to minimize the energy loss in the oxygen exchanger B6. The global transfer coefficients for all the heat exchangers present acceptable values ranging from 550 to 1190 kW/m^2 K. Heat recovery from the exchanger B6 should be envisaged in order to minimize the size of this equipment, as well as the energy loss.

Table 5
Assumptions and optimization results for the reference case SFR-HTE.

SFR assumptions				
Steam temperature at the source outlet (K)		484		
Steam pressure (MPa)		2.0		
Thermal energy cost (€/MW h)		15.6		
Process assumptions				
Electricity cost (€/MW h)		40.0		
Hydrogen outlet pressure (MPa)		3.0		
Results				
Hydrogen mole fraction at the electrolyzer outlet		0.775		
Electric potential in the cell (V)		1.26		
Number of cells		1.03×10^6		
Electrolyzer power (MW)		183		
Heat exchanger power (MW):				
	Bl	11.6	B6	28.3
	B2	2.1	B7	4.1
	B3	0.7	B8	57.9
	B4	17.0		
Overheater SX power (MW)		5.7		
Compressor power (kW)		572		
Equipment investments (excluding the electrolyzer)	M€	14.6		
Cell investment (except replacement) M€		38.8		
Hydrogen purity		99.78%		
Hydrogen production cost (€/kg)		1.9		

The contributions to the energy consumption are presented in Fig. 7. The electric energy is converted into thermal energy grounds by means of the efficiency of the electricity production process, fixed at 39%. As for any electrolysis process, the electricity needed to carry out the electrochemical reaction predominates. The energy for vaporizing the water appears next. For the pumping system, compression and electric overheating of the steam, the needed energy is negligible compared to the previous items.

The hydrogen production cost breakdown shows that the electricity consumption accounts for 77% of the total, while the investment and the thermal energy consumption represent around 12% of the cost each (Fig. 8). From these results, the strong impact of the electricity consumption is confirmed, followed by the impact of thermal energy expenses and investment. In the next paragraphs a sensitivity study of these parameters will be detailed.

As concerns the investment cost, it is mostly composed by the electrolyzer cost when including the replacement expenses (>90% of the investment with the present model). The detailed impact of the electrolyzer investment on the hydrogen production cost will be studied through several parameters. Moreover, it should be kept in mind that the hydrogen production costs are indicative values based on a simplified model considering optimistic assumptions; hence it is strongly recommended not to draw premature conclusions.

With the following parametric studies the influence of diverse parameters will be identified: first the impact of the thermal heat source will be examined and then economic parameters that could help lowering the hydrogen production cost.

5.2. Impact of the thermal energy source on hydrogen production cost

The optimization of the coupling between each thermal energy source and the HTE process is carried out. Assuming a cell current density of 3500 A/m^2 and lifespan of 5 years, we obtained the results presented in Table 6, where the heat source characteristics are also recalled. Furthermore, in Fig. 9 we present the hydrogen production cost classified from the lowest cost to the highest one. The assumptions for operating the biomass incineration units are a biomass-fuel with 10% moisture, 6% of hydrogen content, 19 MJ/kg of High Heating value and a cost of 8.3 €/ton.

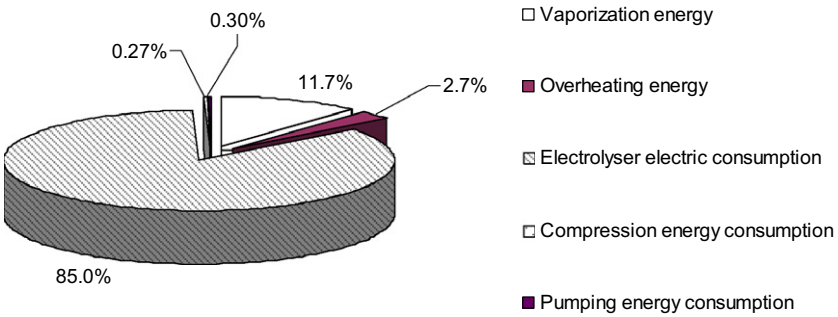

Fig. 7. Energy consumption in the HTE process.

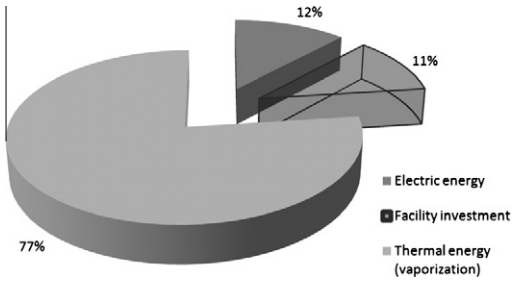

Fig. 8. Hydrogen production cost breakdown.

Despite the gap of the produced steam temperature, the thermal energy source seems not to strongly influence the hydrogen production cost. Moreover, it is also noticed from the results in Table 6 that the temperature at the electrolyzer inlet is quite the same for all the studied couplings. However, a new question arises: why higher steam temperatures lead to higher hydrogen production costs? Domestic waste incineration units present the highest steam temperature and also the highest production cost (cf. Fig. 10).

The plot of the hydrogen production cost against thermal energy cost helps to explain this point (Fig. 11). Besides being characterized by the highest temperature, incineration of domestic waste is the most expensive thermal energy source, consequently leading to a relatively high hydrogen cost. When comparing the SFR and biomass couplings it can be observed that higher temperatures can lead to diminish the production cost if it does not imply greater heat costs. A compromise between low cost thermal energy source and high temperature steam is needed.

As regards the influence of the pressure of the steam generated, the energy needed to reach the pressure at the hydrogen facility outlet seems negligible when compared to other needs. However, we remind that in this work the compressor is increasing only the pressure of the hydrogen stream in up to 1.5 MPa, which is a moderate demand for this equipment.

5.3. Economies-of-scale

As a reference case, a hydrogen production rate of 1.5 kg/s was fixed corresponding to the hydrogen needs of an industrial small unit of ammonia. The impact of increasing the hydrogen production rate on the production cost was evaluated in a range between 1 and 3.5 kg/s that would fit the needs of ammonia plants or refineries. Results in this range vary within ±3% around 1.9 €/kg. HTE is a modular process for the electrolysis part and, as presented before, the electrolyzer investment represents more than 90% of the total equipment expenses. This explains the very limited impact of the plant size on the hydrogen production cost. In order to model the size effect (or in other words the economies-of-scale), the invested capital (I) for each hydrogen production capacity (Cap) was

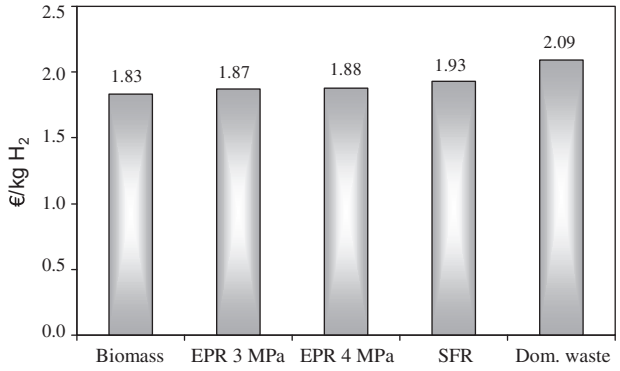

Fig. 9. Hydrogen production cost for different thermal energy sources coupled to the HTE process (electrolysis cell current density = 3500 A/m^2, lifespan = 5 years).

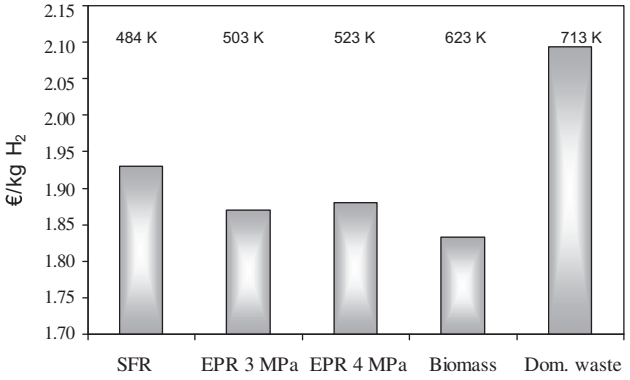

Fig. 10. Hydrogen production cost for different thermal energy sources coupled to the HTE process – ordered according to steam temperatures (electrolysis cells: current density = 3500 A/m^2, lifespan = 5 years).

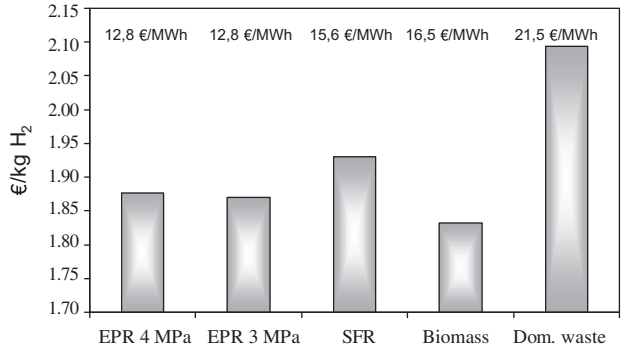

Fig. 11. Hydrogen production cost for different thermal energy sources coupled to the HTE process – ordered according to thermal energy costs (electrolysis cells: current density = 3500 A/m^2, lifespan = 5 years).

Table 6
Optimization results for HTE process coupled to different thermal energy sources.

	SFR	EPR	EPR	Biomass	Domestic waste
Steam temperature (K)	484	523	503	623	713
Steam pressure (MPa)	2.0	4.0	3.0	2.0	4.0
Thermal energy cost (€/MW h)	15.6	12.8	12.8	16.5	21.5
Cell inlet temperature (K)	1076.9	1080.2	1077.5	1077.7	1082.3
Steam sent to exchangers B3 and B4 (ratio of total steam produced by the source)	0.59	0.66	0.56	0.72	0.58
Electric energy cost (€/MW h)	40	40	40	40	40
Hydrogen purity (%vol)	99.78	99.88	99.85	99.89	99.88
Hydrogen pressure (end of process – MPa)	3.0	4.0	3.0	3.0	4.0
Hydrogen production cost (€/kg)	1.93	1.88	1.87	1.83	2.09

plotted against the production capacity of the plant, and fitted by Eq. (19). The exponent $\beta = 0.9855$ (close to 1) was found and reflects that the size effect is very limited, the investment being almost proportional to the plant size.

$$I_1 = I_0\left(\frac{Cap_1}{Cap_0}\right)^{\beta} \tag{19}$$

5.4. Current density on the electrolyzer cells

As for the reference case, we supposed the electrolyzer to be made of cathode supported cells operating at 3500 A/m^2. However, current densities may influence the electrolyzer operating mode, hence we studied a range between 3500 A/m^2 and 8500 A/m^2 in order to measure its impact on the hydrogen production cost [35]. The lower value is frequently found in works dealing with SOFC modeling [11] and the upper value is a safety limit that keeps the cell from rapid degradation [13]. In Fig. 12, the variation of the hydrogen production cost results are presented for an applied current density ranging from 3500–8500 A/m^2.

Increasing the current density leads to decrease the surface needed to produce a certain amount of hydrogen, and it also leads to higher energy losses represented by the overpotentials and drives up the temperature of the gases at the outlet of the cell (exothermal mode). Therefore the energy recovery in the heat exchangers is enhanced (15%), then decreasing the energy needed in the overheaters SX and B-AUX. Consequently, results show that increasing the current density drives the hydrogen production cost down. At 3500 A/m^2, the gases inside the cell cool down (endothermal mode) and then the needed electric potential is driven up along the cell, increasing the power of the electrolyzer (1.2 MW) due to an increase in the free Gibbs reaction energy and ohmic resistance. It also doubles the consumption of energy in the electric overheaters SX and B-AUX.

It should be pointed out that an increase in the current density is likely to rapidly damage the cells [37] and the 5% decrease on hydrogen production cost could easily be counterbalanced by earlier replacements.

5.5. Electrolyzer cell lifespan

Nowadays, the cells used to electrolyze water steam at high temperatures have not met an acceptable lifespan value, working only for some thousands of operating hours and presenting an important decrease in performances during the hydrogen production [37]. Performance decreases also lead to an over consumption of electric energy. These phenomena are not studied here. However, considering that the cell will be replaced anyway after several years, the impact of this replacement on the hydrogen production cost is assessed. Fig. 13 presents the results for a HTE process coupled with the SFR reactor and an electrolyzer made of cathode supported cells. Longer lifespans of course lead to lower production costs. However, after having reached 5 years, the decrease on hydrogen cost is less significant due to discounting effects. For values ranging from 1 to 5 years, this impact is much more important: improving the cell lifespan from 1 to 3 years reduces the hydrogen production cost by 34%, by 5% from 3 to 5 years, and by 8% from 5 to 10 years.

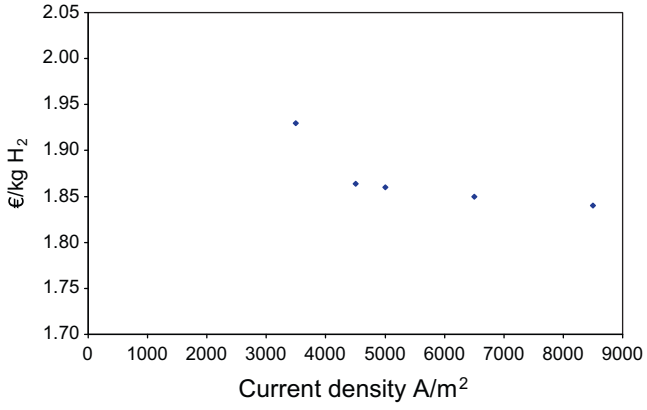

Fig. 12. Hydrogen production cost as a function of the cell current density (cathode supported type).

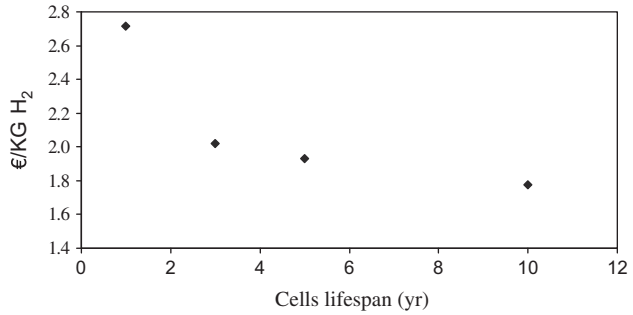

Fig. 13. Hydrogen production cost as a function of the cell investment cost (current density: 3500 A/m^2; plant capacity: 1.5 kg/s).

The investment of the hydrogen facility accounts for almost half of the hydrogen production cost when the cell lifespan is 1 year and its share is then smoothly lowered down to only 8% of the hydrogen cost when the lifespan reaches a value of 10 years. In this last case, the electric energy expenses amount to 82% of the production cost.

5.6. Impact of the cell investment cost

The reference case considers an electrolyzer investment cost of 170 $/kW, which corresponds to target values established by the Department of Energy of the United States [27]. Large production of cells is still not mature and therefore we evaluated the impact of cell costs from this value up to 1000 $/kW. From a technical point of view, results of the optimization show that the operating temperatures remain identical for the whole studied range. Moreover, considering that the investment only represents 12% of the total cost, cell price is expected to have a moderate influence on the hydrogen production cost. In Fig. 14, results confirm that a decrease on the hydrogen production costs happens when the cell cost also decreases. The impact of passing from 1000 $/kW to 170 $/kW only leads to a 25% reduction on hydrogen cost. Further economies and cell cost reduction would indeed drive down the production costs, however only in a moderate way.

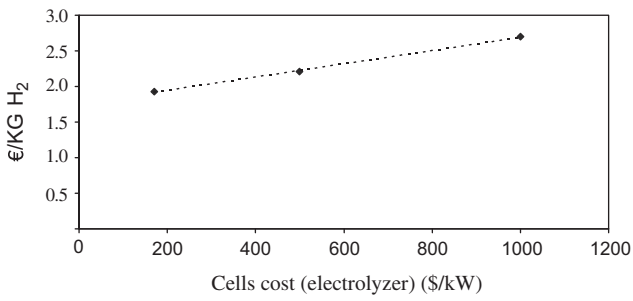

Fig. 14. Hydrogen production cost as a function of the cell investment cost (current density: 3500 A/m^2; plant capacity: 1.5 kg/s).

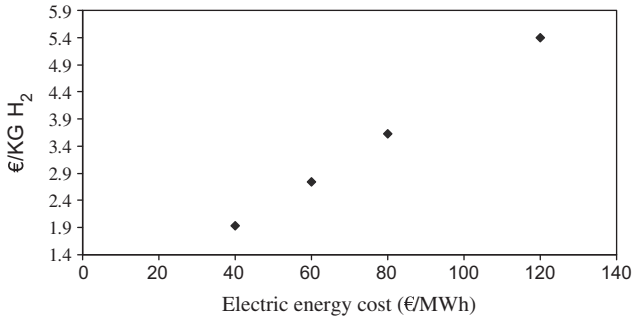

Fig. 15. Hydrogen production cost as a function of electricity cost.

5.7. Electric energy cost

As it was previously stated, to estimate hydrogen production costs we assumed an electricity production cost of 40 €/MW h. This value arises from literature data for Nuclear Reactors in 2003 at 28.4 €/MW h, 22–35 €/MW h in 2005 and the EPR electricity production value estimated at 43 €/MW h (also 2005) [38–39]. Market electricity prices are higher than 40 €/MW h and would strongly influence the hydrogen production cost, as shown in Fig. 15. Passing from 40 to 60 €/MW h, the hydrogen production cost would rise of 42%.

5.8. Impact of the cell support (cathode or electrolyte supported)

In previous paragraphs, the influence of increasing the current density in the cell was explained, as well as the possible impact of shorter life spans on the hydrogen production cost. To finish with, in this section we focus on the results on the operating parameters and hydrogen cost when electrolyte and cathode supported cells are confronted. Because of the intrinsic characteristics of these cells, basically ohmic resistance, the electrolyte supported cells shift from endothermal to iso and exothermal mode in a narrower and lower range of current densities than cathode supported cells. Assuming that manufacturing costs are identical for both kinds of cells, results will show that the hydrogen cost profiles remain similar at the same point of endo/iso/exothermicity, whatever the cell is (Fig. 16).

The decrease on hydrogen production cost by shifting from endo to exothermal mode is almost equivalent to 5%, as presented in Section 5.4. However, specific technical issues arise: electrolyte supported cells operate at lower current densities, their lifespan would perhaps be enhanced and the hydrogen production cost would then be driven down. Nevertheless, the surface (or the number of cells) needed to produce 1.5 kg/s of hydrogen with an electrolyzer made of cathode supported cells is estimated to be at least half the one needed for an electrolyte supported electrolyzer (due to differences of current densities).

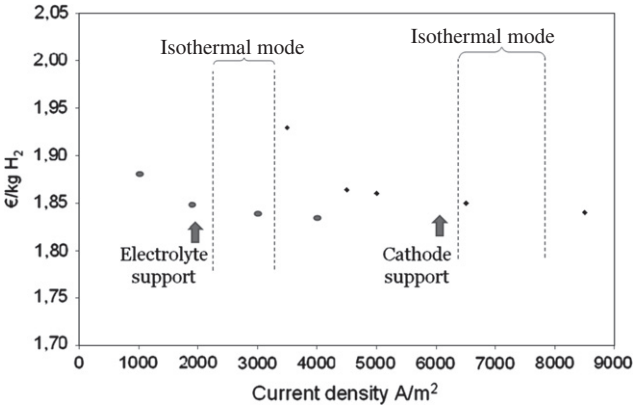

Fig. 16. Hydrogen production cost for cathode and electrolyte supported cell electrolyzers, lifespan of 5 years, as a function of the current density.

6. Conclusion

Massive hydrogen production by High Temperature Electrolysis could be envisaged considering the use of other thermal energy sources rather than only high temperature nuclear reactors. In this work, we present the coupling of the HTE process to medium temperature sources that exclusively supply the energy needed to vaporize the water to be converted into hydrogen. Economic competitiveness seems achievable if several R&D steps are reached. Let us recall here that the techno-economic model is a simplified one, hence only trends are given.

The thermal energy source needs to achieve a compromise between low costs and high temperatures, but it is not compulsory since the influence of the heat source on the hydrogen production cost is limited. An overall deviation of ±8% was found on the results for the sources here presented.

Concerning the cell performances, operating parameters leading to an exothermal mode in the electrolyzer cells (i.e. high current densities) seem more efficient towards low production costs. However, the lifespan would probably be diminished and this could lead to a sharp increase on hydrogen production cost. The use of electrolyte supported cells could be considered as a first step for industrialization of HTE if they reach an acceptable lifespan, around 3 years, since the electrolyzer surface presents a moderate effect on production costs. Moreover, the cell investment cost presents a moderate influence on hydrogen production cost. The target value established at 170 $/kW could certainly lead to low production costs, but the installation costs need to be investigated. Besides, as shown before and quite logically, hydrogen production cost is very sensitive to electricity costs. Therefore, the business model is of great importance when evaluating electrolysis-based processes.

References

[1] Doenitz W, Hermeking H, Kitzmann I, Koch A, Roettenbacher R, Schaefer W, et al. High temperature water vapor electrolysis (HOT ELLY). Germany (FR): Final Report Dornier-Werke G.m.b.H., Friedrichshafen; 1980.
[2] Utgikar V, Thiesen T. Life cycle assessment of high temperature electrolysis for hydrogen production via nuclear energy. Int J Hydrogen Energy 2006;31(7):939–44.
[3] Lattin WC, Vivek P, Utgikar V. Global warming potential of the sulfur–iodine process using life cycle assessment methodology. Int J Hydrogen Energy 2009;34(2):737–44.
[4] Holladay JD, Hu J, King DL, Wang Y. An overview of hydrogen production technologies. Catal Today 2009;139(4):244–60.
[5] Herring JS, O'Brien JE, Stoots CM, Hawkes GL, Hartvigsen JJ, Shahnam M. Progress in high-temperature electrolysis for hydrogen production using planar SOFC technology. Int J Hydrogen Energy 2007;32(4):440–50.
[6] O'Brien JE, Stoots CM, Hartvigsen JJ, Herring JS. Performance of planar high-temperature electrolysis stacks for hydrogen production from nuclear energy. In: International topical meeting on nuclear reactor thermal hydraulics no. 11; 2007, vol. 158(2). p. 118–31 [Avignon, France (02/10/05)].
[7] Sigurvinsson J, Mansilla C, Lovera P, Werkoff F. Can high temperature steam electrolysis function with geothermal heat? Int J Hydrogen Energy 2007;32(9):1174–82.
[8] McKellar MG, O'Brien JE, Herring JS. Commercial scale performance predictions for high temperature electrolysis plants three advanced reactor types. DOE/INL-EXT 07 13575; 2007.
[9] Herring JS, O'Brien JE, Stoots SM, Hartvigsen JJ, Petri MC, Carter JD et al. Overview of high-temperature electrolysis for hydrogen production. INL/CON-07-12192, USA; June 2007.
[10] Paul-Joseph J. Economic evaluation of the HTE process-additional layout and design of the process. Report CEA/DEN/DTN/STPA/LPC/2007/030 19/06/2007.
[11] Carles P, Le Duigou A, Lovera P, Rodriguez G, Gilardi T, Paul-Joseph J et al.. Preliminary study of HTE process coupled with a nuclear reactor, Report. CEA – 2007, RT DPC/DIR 07-001.

[12] Fujiwara S, Kasai S, Yamauchi H, Yamada K, Makino S, Matsunaga K, et al. Hydrogen production by high temperature electrolysis with nuclear reactor. Prog Nucl Energy 2008;50(2–6):422–6.
[13] Rivera-Tinoco R, Mansilla C, Bouallou C, Werkoff F. On the possibilities of producing hydrogen by high temperature electrolysis of water steam supplied from biomass or waste incineration units. Int J Green Energy 2008;5(5):388–404.
[14] Rivera Tinoco R, Mansilla C, Werkoff F, Bouallou C. Techno-economic study of hydrogen production by high temperature electrolysis coupled with an EPR, SFR or HTR – water steam production and coupling possibilities. Int J Nucl Hydrogen Prod Appl 2008;1(3):249–66.
[15] Haubensack D. Energy conversion cycles for RNR-Na, CEA/DEN/CAD/DER/SESI/LCSI/NT/DR 8 08/02/08. Confidential document CEA; 2008.
[16] Zrodnikov AV, Toshinsky GI, Komlev OG, Dragunov YG, Stepanov VS, Klimov NN, et al. Nuclear power development in market conditions with use of multi-purpose modular fast reactors SVBR-75/100. Nucl Eng Des 2006;236:1490–502.
[17] Tucek K, Carlsson J, Wider H. Comparison of sodium and lead-cooled fast reactors regarding reactor physics aspects, severe safety and economical issues. Nucl Eng Des 2006;236:1589–98.
[18] Chauvel A, Fournier G, et Raimbault C. Handbook of process economics. France: Publications de l'Institut Français du Pétrole, Editions Technip; 2001.
[19] Stoots CM, O'Brien JE, McKellar MG, Hawkes GL, Herring SJ. Engineering process model for high-temperature electrolysis system performance evaluation. AIChE 2005 annual meeting; November 2005.
[20] Ni M, Leung MKH, Leung DYC. Technological development of hydrogen production by solid oxide electrolyzer cell (SOEC). Int J Hydrogen Energy 2008;33(9):2337–54.
[21] Jensen SH. Durability of solid oxide electrolysis cells for hydrogen production. Department of Solid State Chemistry and Fuel Cells, Risø-1608 (EN); 2008.
[22] Ni M, Leung MKH, Leung DYC. A modeling study on concentration overpotentials of a reversible solid oxide fuel cell. J Power Sour 2006;163:460–6.
[23] CSIRO MMT Brochures – Technologies Hydrogen Economy Technologies; 2009. <http://www.cmit.csiro.au/brochures/tech/hydrogen/>.
[24] Hartvigsen J, Swank D, Schade C, Bordia R. Large area cell for hybrid hydrogen co-generation process. US DOE hydrogen program, FY progress report;2005.
[25] Balachov II, Crouch-Baker S, Hornbostel M, McKubre M, Sanjurjo A, Tanzella F. Modular system for hydrogen generation and oxygen recovery. US DOE hydrogen program, FY progress report; 2005.
[26] Rivera Tinoco, R. Techno-economic study of hydrogen production by high temperature electrolysis coupled with different thermal energy sources, Mines ParisTech. PhD thesis, France; 2009.
[27] Thijssen J. The impact of scale-up and production volume on SOFC manufacturing cost. DOE/NETL; 2007.
[28] Greth Technical handbook. Pressure drop and simple phase heat transfer in plate exchangers, Greth document confidential; 2009.
[29] Mansilla C, Sigurvinsson J, Bontemps A, Maréchal A, Werkoff F. Heat management for hydrogen production by high temperature steam electrolysis. Energy 2007;32(4):423–30.
[30] Perry, S. Heat exchangers, chemical engineering handbook, 7th ed. Mc Graw Hill; 1997. p. 11–52.
[31] Le Duigou A, Lovera P. High temperature electrolysis: process flowsheets, CEA/DEN/DANS/DPC/SCP/06-DO-62. Document interne; November 2006.
[32] Simpson R, Abakarov A, Teixeira A. Variable retort temperature optimization using adaptive random search techniques. Food Control 2008;19(11):1023–32.
[33] Salcedo R, Gonçalves MJ, Feyo de Azevedo S. An improved random-search algorithm for non-linear optimization. Comput Chem Eng 1990;14(10):1111–26.
[34] Arnaud G, Dumas M. Vizir handbook (genetic algorithm program). Report CEA DM2S SFME/LETR/RT/04-013/A. France; 2004.
[35] Ni M, Leung MKH, Leung DYC. Parametric study of solid oxide steam electrolyser for hydrogen production. Int J Hydrogen Energy 2007;32:2305–13.
[36] Udagawa J, Aguiar P, Brandon NP. Hydrogen production through steam electrolysis: model-based steady state performance of a cathode-supported intermediate temperature solid oxide electrolysis cell. J Power Sour 2007;166:127–36.
[37] Brisse A, Schefold J, Zahid M. High temperature water electrolysis in solid oxide cells. Int J Hydrogen Energy 2008;33(20):5375–82.
[38] DGEMP-DIDEME. Reference costs for electricity generation. Secrétariat d'Etat à l'Industrie – Ministère de l'Economie, des Finances et de l'Industrie, France; 2003.
[39] Forecast Costs for Electricity Production. OECD, Agence Internationale de l'Energie Atomique (IAEA). ISBN: 9789264008298; 2005.